

# The AGN Hubble Diagram and Its Implications for Cosmology

Fulvio Melia<sup>1</sup>

Department of Astronomy, the Applied Math Program, and Department of Physics  
The University of Arizona  
Tucson, AZ 85721

E-mail: [fmelia@email.arizona.edu](mailto:fmelia@email.arizona.edu)

**Abstract.** We use a recently proposed luminosity distance measure for relatively nearby active galactic nuclei (AGNs) to test the predicted expansion of the Universe in the  $R_h = ct$  and  $\Lambda$ CDM cosmologies. This comparative study is particularly relevant to the question of whether or not the Universe underwent a transition from decelerated to accelerated expansion, which is believed to have occurred—on the basis of Type Ia SN studies—within the redshift range ( $0 \lesssim z \lesssim 1.3$ ) that will eventually be sampled by these objects. We find that the AGN Hubble Diagram constructed from currently available sources does not support the existence of such a transition. While the scatter in the AGN data is still too large for any firm conclusions to be drawn, the results reported here nonetheless confirm and strengthen similar results of comparative analyses using other types of source, such as cosmic chronometers and gamma ray bursts. We show that the Akaike, Kullback, and Bayes Information Criteria all consistently yield a likelihood of  $\sim 74 - 93\%$  that  $R_h = ct$  is closer to the “true” cosmology than  $\Lambda$ CDM is.

---

<sup>1</sup>John Woodruff Simpson Fellow.

---

## Contents

<b>1</b>	<b>Introduction</b>	<b>1</b>
<b>2</b>	<b>A Distance Measure Using AGNs</b>	<b>2</b>
<b>3</b>	<b>Theoretical Fits to the AGN Hubble Diagram</b>	<b>4</b>
<b>4</b>	<b>Discussion</b>	<b>7</b>
<b>5</b>	<b>Conclusions</b>	<b>9</b>

---

## 1 Introduction

A proposal was made recently to infer accurate luminosity distances to Active Galactic Nuclei (AGNs) using the tight relationship (established via reverberation mapping) between the luminosity of their central engine and the radius of the broad-line region (BLR [1]). If feasible, this technique would open up the possibility of examining the cosmological expansion out to a redshift  $z \sim 2 - 3$  using a class of objects other than the already well known and studied Type Ia supernovae [2, 3].

Finding reliable distance measures beyond the reach ( $z \sim 2$ ) of current tools is difficult, but several methods have been proposed in the past few years. We recently added some support to the idea of using gamma ray burst sources (GRBs) to construct a Hubble Diagram (HD) out to redshifts  $z \sim 5 - 6$  [4], using correlations among certain spectral and lightcurve features as luminosity indicators. Using the most up-to-date GRB sample appropriate for this work, we showed that the GRB HD produces fits useful in delimiting the possible expansion scenarios in this redshift range, though  $\sim 20\%$  of the events lie at least  $2\sigma$  away from the best-fit curves, suggesting that either some contamination by non-standard GRB luminosities is unavoidable, or that the errors and intrinsic scatter are still being underestimated. This class of sources will no doubt become increasingly important as the precision of their measured properties continues to improve, but there is clearly still a need to search for other possibilities.

In another study, closely related to the subject of this paper, we also proposed the use of high- $z$  quasars to construct an HD at redshifts  $z \gtrsim 6 - 7$  [52]. The use of high- $z$  quasars as standard candles has recently been made possible by the recognition that a single observation of the quasar's spectrum can yield both its optical/UV luminosity—and therefore the distance of line-emitting gas from the central ionizing source—and the width of BLR lines, such as Mg II—which facilitates a measurement of the velocity of the line-emitting gas. Together, these data can, in principle, provide an accurate determination of the black hole's mass. And since it is becoming more and more evident that quasars at  $z \gtrsim 6$  are accreting at close to their Eddington limit [6, 7], it may be possible to base the high- $z$  quasar HD on the assumption that the luminosity function at these high redshifts is well constrained.<sup>1</sup> A second important discovery making it possible to study high- $z$  quasars in

---

<sup>1</sup>As we shall see shortly, this approach is quite different from that suggested for nearby AGNs, even though both make use of our knowledge concerning the BLR. The high- $z$  quasar technique is, by necessity, statistical in nature, whereas the nearby AGN method relies on the measurement of fluxes and time lags in individual sources.

this fashion was the identification of quasar ULAS J1120+0641 at  $z = 7.085$  [8], which has significantly extended the redshift range of these sources, providing essential leverage when fitting theoretical luminosity distances to the data.

Since their discovery in the early 1960’s, many attempts have been made to use AGNs as standard candles [9–12]. None of these were very successful, but the aforementioned improvements in our understanding of the BLR have dramatically changed this situation. In §2 of this paper, we will describe the method suggested by Watson et al. [1] to construct the nearby AGN HD, and then apply it to test the predictions of several cosmological models in §3. One of our primary goals will be to compare the  $R_h = ct$  Universe directly with  $\Lambda$ CDM in the very important redshift range  $0 \lesssim z \lesssim 2$ , where the best evidence for a transition from cosmic deceleration to acceleration is claimed to have been found. We will discuss the consequences of our results in §4.

## 2 A Distance Measure Using AGNs

Reverberation mapping [13] relies on high-quality spectrophotometric monitoring of an AGN over an extended period of time (in many cases lasting several years). The BLR lines are due to photoionization by the hot accretion disk surrounding the black hole, which produces a variable continuum flux. Because of the close physical link between the two regions, these variations are echoed after a light-crossing time by changes in the flux of the broad emission lines. This technique provides a probe into regions only  $\sim 0.01$  pc in extent at the centers of arbitrarily distant galaxies. As of today, reverberation mapping has yielded black-hole masses for over 50 AGNs [14–16].

The size  $R$  of the BLR is determined by the depth to which the gas surrounding the black hole can be photoionized by the central continuum source. Therefore, one would expect that  $R \propto \sqrt{L}$  [17–19]. In addition, simple light-travel time arguments suggest that  $R \sim \tau c$ , where  $\tau$  is the lag time between variations in the continuum and the response (or echo) measured with the broad lines (typically H $\beta$  or C IV). Thus, the observable quantity  $\tau/\sqrt{F}$ , where  $F$  is the measured AGN continuum flux, should be proportional to the luminosity distance to the source, i.e.,

$$d_L \propto \frac{\tau}{\sqrt{F}}. \quad (2.1)$$

Note, in particular, that no cosmological model is assumed in order to extract this information from the data. Both  $\tau$  and  $F$  are quantities that can be observed directly, independently of the background expansion, when the appropriate (measured) cosmological redshift is taken into account for the purpose of making rest-frame measurements.

Recent improvements in the measurement of  $\tau$  and  $F$  have led to a confirmation that the radius-luminosity relationship follows the simple law implied by Equation (2.1) across four orders of magnitude in  $L$  [15, 20]. Chief among these was the successful removal of the contaminating effects of the host galaxy, making measurements of the lag time more precisely by re-observing AGNs with poorly sampled light curves, and filling in the low-luminosity end of the sample.

Our sample of 35 observed  $\tau/\sqrt{F}$  values is taken from ref. [1], who compiled all the available lags for the H $\beta$  line and rest-frame 5100 Å continuum fluxes (e.g., from refs. [15, 21]). As mentioned above, the removal of the host galaxy flux from the continuum measurement is critical, and was done primarily using images from the *Hubble Space Telescope* to model the contribution from the underlying host galaxy [15]. In addition, Watson et al. [1] corrected the

fluxes for Galactic extinction (see also refs. [22, 23]), though internal extinction corrections are not available for enough of the 35 sources in this sample to be applied uniformly (more on this below).

The broad emission lines necessary for this kind of work are characteristic of the spectra of near-face-on AGNs, such as Seyfert 1 galaxies. However, the relationship between the size of the BLR and the central continuum luminosity is dependent only upon the depth to which the surrounding medium can be photoionized. The current sample of AGNs, assembled from all available lags in the  $H\beta$ -line and rest-frame 5100 Å continuum fluxes, exhibits a tight radius-luminosity relationship indicating that the ionization parameter and the gas density are both close to constant across all 35 objects. The fact that the former is constant is not surprising based on the locally optimally emitting cloud model [24], but the mechanism that keeps the density close to the same value in the BLR across sources, and for a wide range of luminosities, is not yet understood. The variation of this gas density away from a constant value will ultimately be the factor that limits the accuracy of the AGN HD. For the foreseeable future, however, it appears that the observational uncertainties will dominate the scatter.

These data are shown in Figure 1, together with the best fit curves from several cosmological models, which we will discuss in the next section. The lags for most of these objects were recalculated by Zu et al. [20] using the stochastic process estimation for AGN reverberation (SPEAR). One of the objects, NGC 7469, was found to have a significantly discrepant lag. Its current position on the diagram (Figure 1) is based on the updated measurement in ref. [20], rather than from the original set of observations.

The other named galaxies in this plot were special in one or more ways for the compilation of this sample. At this time, only NGC 3227 and NGC 4051 have direct distance estimates. Since the Tully-Fisher distance to NGC 4015 is the less accurate of the two, the  $\tau/\sqrt{F}$  distance relation was calibrated to the luminosity distance of galaxy NGC 3227 (see also ref. [25]). Nonetheless, the uncertainty in this calibration is relatively large, but NGC 4051 and NGC 3227 are close enough that eventually Cepheid-derived distances will provide a better absolute calibration.

The source NGC 5548 demonstrates the benefit to be gained from repeated reverberation measurements, which substantially refines the distance to any of these objects. The observational uncertainty for this AGN is 0.05 dex (0.13 mag) after about a dozen such observations; it is typically  $\sim 0.14$  dex (0.35 mag) for sources with a single measurement. Some flux variation in the continuum over a measurable time  $\tau$  is necessary in order to infer the time delay in the signal reaching the BLR, where the change is echoed in the lines. But large flux variations over a time that would affect their location  $R$  would also be known within this  $\tau$ , and these are not observed. Indeed, for those systems that have been observed repeatedly, very little intrinsic variation has been seen in  $\tau/\sqrt{F}$ , suggesting that flux variability contributes much less than measurement uncertainties to the overall scatter.

Finally, a likely source of scatter is due to extinction associated with the AGN and its host galaxy. To illustrate how significant this effect can be, Figure 1 also highlights the position of NGC 3516, which currently lies more than  $1\sigma$  away from the best-fit curves. However, an application of the recently measured extinction correction [21] would shift it to a position very close to these curves. But since very few extinction corrections are known, we are not including them for the current version of this compilation. It has been estimated [1] that the overall scatter may be reduced by as much as  $\sim 0.08$  dex (0.2 mag) with the accurate correction of all of the internal extinctions. Unfortunately, only a handful of the AGNs in the sample used here have sufficient data for the internal AGN and host-galaxy extinction to be

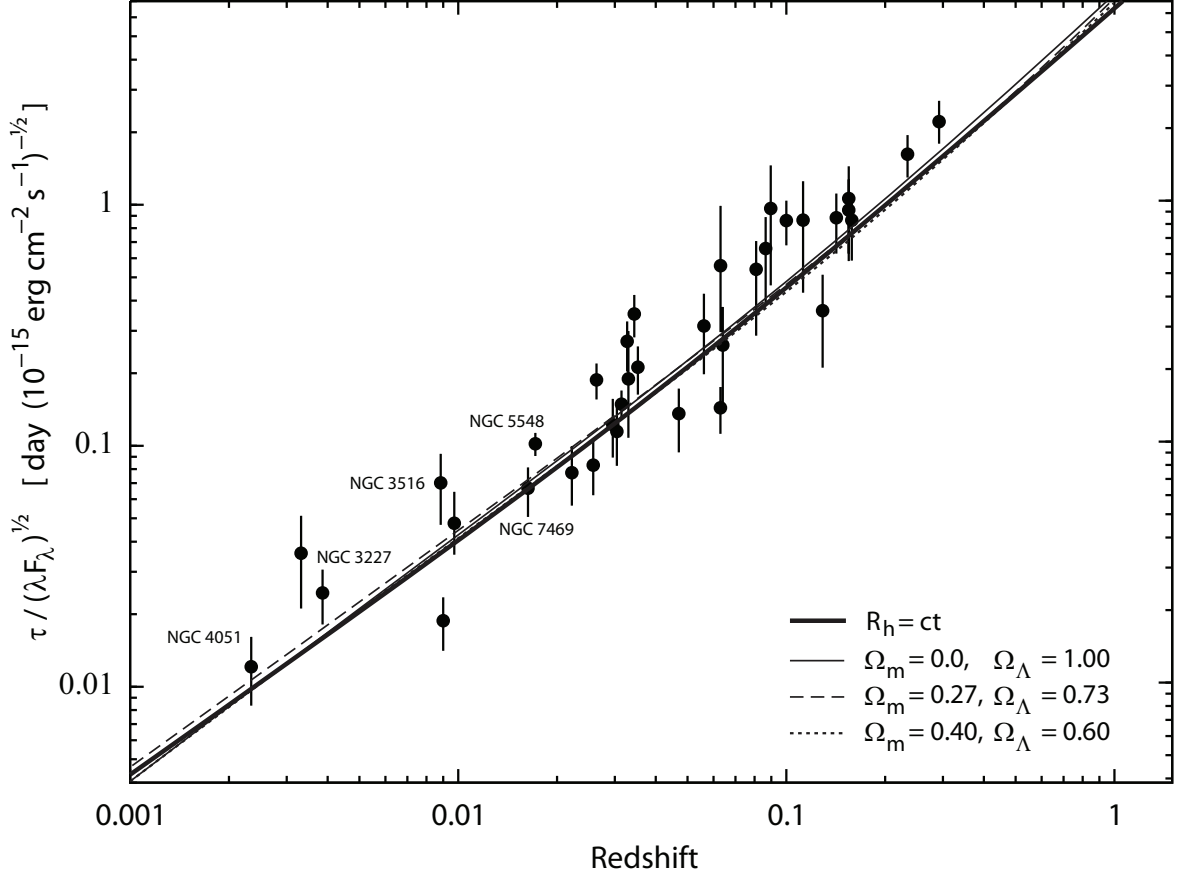


**Figure 1.** Hubble Diagram constructed from the AGN sample in ref. [1]. The position of NGC 7469 is based on Zu et al.’s (2011) re-measurement of the time lags in this source using the SPEAR method. The vertical axis shows the luminosity distance indicator  $\tau/\sqrt{F}$  (see Equation 2.1), versus redshift for all the AGNs with  $H\beta$  measurements. Also shown are the best fit curves for the  $R_h = ct$  Universe ( $\chi_{\text{dof}}^2 = 2.85$  for 34 degrees of freedom), and the optimized  $\Lambda$ CDM model (*thin, solid* curve;  $\chi_{\text{dof}}^2 = 2.97$  for 32 degrees of freedom), and two other variations of the standard model (both with  $\chi_{\text{dof}}^2 = 3.01$  for 32 degrees of freedom). The best fit  $\Lambda$ CDM model has  $w_\Lambda = -1$ . For the sake of comparison, the other two variations of the standard model also have  $w_\Lambda = -1$ . In addition, the  $\Lambda$ CDM model with  $\Omega_m = 0.27$  has  $H_0 = 74.9_{-5.4}^{+5.3}$  km s $^{-1}$  Mpc $^{-1}$  (2 model parameters and 1- $\sigma$  errors calculated as shown in Figures 2 and 3), while the model with  $\Omega_m = 0.40$  has  $H_0 = 75.0_{-5.6}^{+4.8}$  km s $^{-1}$  Mpc $^{-1}$ .

estimated at the present time. And in most of those cases (with the exception of NGC 3516), the discrepancy between estimates made in a single object are as large as the extinction correction itself (see, e.g., refs. [15, 21, 26]).

### 3 Theoretical Fits to the AGN Hubble Diagram

Depending on how one chooses to characterize the dark energy and its equation-of-state  $p_\Lambda = w_\Lambda \rho_\Lambda$ ,  $\Lambda$ CDM can have as many as 7 free parameters, including the Hubble constant  $H_0$ , the matter energy density  $\Omega_m \equiv \rho_m/\rho_c$  normalized to today’s critical density  $\rho_c \equiv (3c^2/8\pi G)H_0^2$ , the similarly defined dark energy density  $\Omega_\Lambda$ , and  $\Omega_k$ , representing the spatial curvature of

the Universe—appearing as a term proportional to the spatial curvature constant  $k$  in the Friedmann equation. In this paper, we will take the minimalist approach and consider only the most essential parameters needed to fit the AGN data. For this purpose, we will take guidance from other observations (such as those with WMAP and *Planck*), which indicate that  $k = 0$  (i.e., that the Universe is spatially flat). In other words, we will treat  $k$  as a prior and not include it in the optimization procedure, which means that  $\Omega_m + \Omega_\Lambda = 1$  in the redshift range of interest. As such, the  $\Lambda$ CDM model we use here for comparison with the  $R_h = ct$  Universe is characterized by three essential parameters:  $H_0$ ,  $\Omega_m$  and  $w_\Lambda$ , with the additional restriction that the Universe has no phantom energy, i.e., that  $w_\Lambda \geq -1$ .

In fitting the AGN data in Figure 1, we will compare the predictions of  $\Lambda$ CDM with those of the  $R_h = ct$  Universe. Both models are Friedmann-Robertson-Walker cosmologies, but  $R_h = ct$  and  $\Lambda$ CDM handle  $\rho$  differently. The theoretical basis for the former is rather straightforward [27, 28] and stems directly from the fact that the condition  $R_h = ct$ , equating the Universe’s gravitational horizon (equal to the Hubble radius) to the distance light could have traveled since the big bang, is required by the simultaneous application of both the Cosmological principle and Weyl’s postulate [29]. This constraint forces the expansion factor  $a(t) \propto t$ , which requires a total equation-of-state  $p = -\rho/3$ , in terms of the total pressure  $p$  and density  $\rho$ . Whereas  $\Lambda$ CDM guesses the constituents of  $\rho$  (matter, radiation, dark energy) and their individual equations-of-state, from which the dynamics ensues, the expansion history in  $R_h = ct$  is known precisely at all cosmic times  $t$ . And the various constituents must partition themselves in such a way as to always preserve the overall condition  $p = -\rho/3$ .

The observables in  $R_h = ct$  take on simple analytic forms. For example, the luminosity distance is given by the elegant expression<sup>2</sup>

$$D_L^{R_h=ct} = \frac{c}{H_0}(1+z)\ln(1+z) \quad (3.1)$$

which, unlike  $\Lambda$ CDM, has only one free parameter—the Hubble constant  $H_0$ . The factor  $c/H_0$  is in fact the gravitational horizon  $R_h(t_0)$  at the present time, so we may also write the luminosity distance as

$$D_L^{R_h=ct} = R_h(t_0)(1+z)\ln(1+z). \quad (3.2)$$

By comparison, the luminosity distance in  $\Lambda$ CDM is given as

$$D_L^{\Lambda\text{CDM}}(z) = \frac{c}{H_0} \frac{(1+z)}{\sqrt{|\Omega_k|}} \text{sinn} \left\{ |\Omega_k|^{1/2} \times \int_0^z \frac{dz}{\sqrt{\Omega_m(1+z)^3 + \Omega_\Lambda(1+z)^{3(1+w)}}} \right\}, \quad (3.3)$$

where  $c$  is the speed of light. (Note that the fractional density  $\Omega_r$  due to radiation is insignificant compared to the other components, and is ignored in this expression.) The function  $\text{sinn}$  is  $\sinh$  when  $\Omega_k > 0$  and  $\sin$  when  $\Omega_k < 0$ . Since we take the Universe to be flat with  $\Omega_k = 0$ , Equation (3.3) simplifies to the form  $(1+z)c/H_0$  times the integral.

In Figure 1, the best fit models calculated from Equation (3.2), in the case of  $R_h = ct$ , and Equation (3.3), for  $\Lambda$ CDM, are shown as solid curves. The Hubble constant in the case of the former has the value  $73.2_{-3.5}^{+3.7}$  km s<sup>-1</sup> Mpc<sup>-1</sup>, with a corresponding reduced  $\chi_{\text{dof}}^2 = 2.85$  (and 34 degrees of freedom). The quality of the fit is shown as a function of  $H_0$

---

<sup>2</sup>The Milne Universe [30] is sometimes confused with  $R_h = ct$ , but in fact its observables are quite different—and have already been refuted by the observations. Unlike the  $R_h = ct$  Universe, in which the spatial curvature constant is  $k = 0$ , the Milne universe is empty and has  $k = -1$ . As a result, the luminosity distance in Milne is  $d_L^{\text{Milne}} = R_h(t_0)(1+z)\sinh[\ln(1+z)]$ , which is not at all consistent with the data [28].

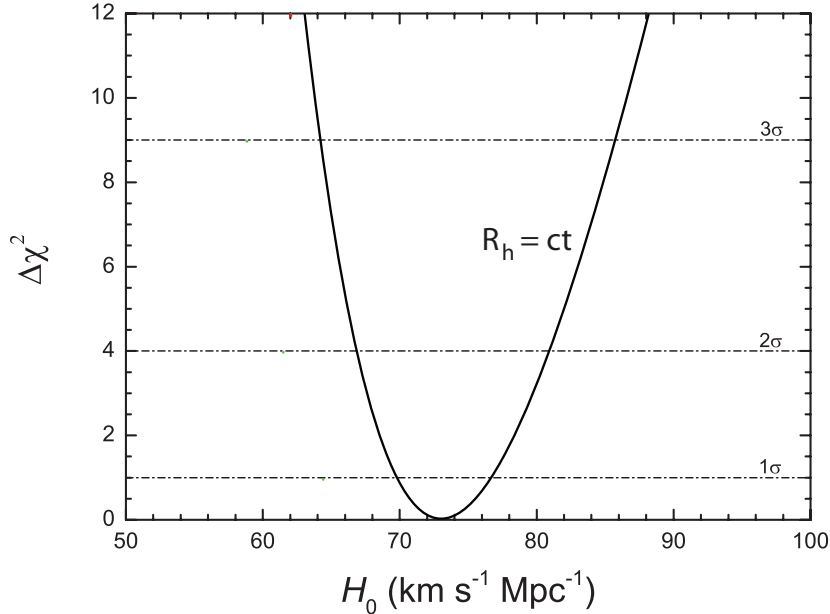


**Figure 2.** Constraints on the Hubble constant,  $H_0$ , for the  $R_h = ct$  Universe, based on fits to the data shown in Figure 1. The optimized Hubble constant has a value  $73.2^{+3.7}_{-3.5}$   $\text{km s}^{-1} \text{Mpc}^{-1}$  (68.3% level of confidence).

in Figure 2, along with the 1, 2 and 3  $\sigma$  levels of confidence. This value is consistent with previous measurements of the Hubble constant, e.g.,  $73.8 \pm 2.4$   $\text{km s}^{-1} \text{Mpc}^{-1}$  reported in ref. [31], though only marginally consistent with the Planck 2013 measurement of  $67.3 \pm 1.2$   $\text{km s}^{-1} \text{Mpc}^{-1}$  [32]. We emphasize that this is the only free parameter available to the  $R_h = ct$  Universe. With the conditions and constraints described above, the best-fit  $\Lambda$ CDM model has the parameter values  $H_0 = 75.0$   $\text{km s}^{-1} \text{Mpc}^{-1}$ ,  $\Omega_m = 0$ , and  $w_\Lambda = -1$ , with a corresponding  $\chi^2_{\text{dof}} = 2.97$  (and 32 degrees of freedom). We note, however, that very similar fits, characterized by comparable  $\chi^2_{\text{dof}}$ 's, may be obtained for  $\Lambda$ CDM using a wide range of parameter values, as indicated in Figure 3, which shows the 1, 2, and 3- $\sigma$  confidence regions for a two-dimensional optimization in  $\Lambda$ CDM, with the adoption of prior values for  $w_{\text{de}}$  and  $\Omega$ . To illustrate this point, we also show in Figure 1 two other  $\Lambda$ CDM models, both with  $\chi^2_{\text{dof}} = 3.01$ , and the parameters indicated in the figure caption. In particular, the model with  $\Omega_m = 0.27$  comes very close to the WMAP-concordance model [33], giving confidence that the use of AGNs to construct a Hubble diagram is meaningful.

We have also attempted to fit the data in Figure 1 using a variation of  $\Lambda$ CDM without assuming flatness. For the Planck 2013 parameter values  $H_0 = 67.3$   $\text{km s}^{-1} \text{Mpc}^{-1}$  and  $\Omega_m = 0.315$ , the best fit corresponds to  $\Omega = 1.24^{+0.19}_{-0.16}$  (1- $\sigma$  errors) and  $w_{\text{de}} = -1$  (this value can range anywhere from 0 to  $-1$  within 1- $\sigma$ ), with a reduced  $\chi^2_{\text{dof}} = 2.91$  (33 degrees of freedom). The quality of this fit is comparable to the others shown in Figure 1, so here too the AGN data are not yet precise enough to rule out a negative spatial curvature, though they do appear to disfavour a closed universe.

The  $\chi^2$  values in the case of  $\Lambda$ CDM are very similar to those reported in ref. [1], who discussed the possible reasons for such large  $\chi^2$ 's and the likely dominant contributions to the scatter in the AGN data shown in Figure 1. The statistical quality of the measurements can

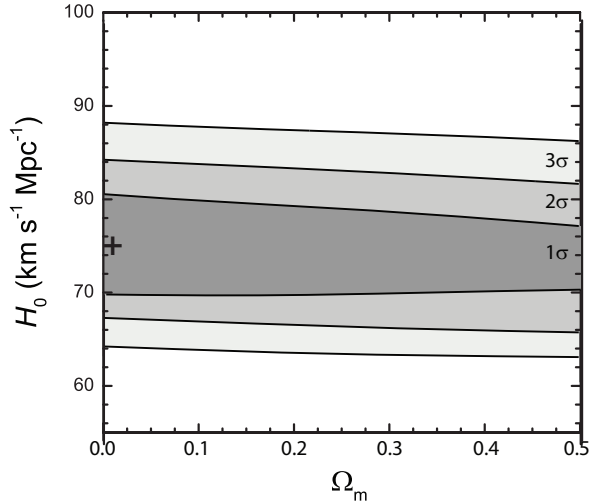


**Figure 3.** One-, two-, and three- $\sigma$  confidence regions for a two-dimensional optimization of the parameters  $H_0$  and  $\Omega_m$  in  $\Lambda$ CDM, with a fixed value  $w_{\text{de}} = -1$  and zero spatial curvature ( $\Omega = 1$ ). The cross indicates the parameter values corresponding to the best-fit. As discussed in the text,  $\Omega_m$  is not yet well constrained by the AGN sample shown in Figure 1.

be improved with an increased number of observations per source, the acquisition of more reliable lags, and better extinction estimates, all of which could decrease the scatter in the AGN HD substantially. The claim is that within a few years of observing, the total scatter could be reduced to levels comparable to those of current Type Ia SN samples [34, 35].

## 4 Discussion

The comparison between  $R_h = ct$  and  $\Lambda$ CDM emerging from Figure 1 suggests that the projected improvements in the AGN HD are important for several reasons. Unless these results change qualitatively when the sample size and quality improve over the coming years,  $R_h = ct$  appears to be a better fit than  $\Lambda$ CDM to the AGN data.

In recent years, we have carried out this kind of comparative analysis between the two cosmologies using a diverse range of observational data, at both low and high redshifts. Since the formulation of measurable quantities, such as the luminosity distance in Equations (3.2) and (3.3), is different in  $R_h = ct$  and  $\Lambda$ CDM, the process of selecting the most likely correct model must also take into account the number of free parameters. The likelihood of either cosmology being closer to the “truth” may be determined from the model selection criteria described in ref. [36]. The Akaike Information Criterion (AIC) [37–39] prefers models with few parameters to those with many, unless the latter provide a substantially better fit to the data. This avoids the possibility that by using a greater number of parameters, one may simply be fitting the noise.

Information criteria were invented specifically to provide a statistical basis for preferring one model over another when their numbers of parameters are different. The fundamental problem is that the introduction of extra parameters will allow an improved fit to the dataset, regardless of whether or not those new parameters are actually relevant. A simple comparison of the maximum likelihood of different models will therefore always favor the model with more parameters. The information criteria were designed to compensate for this by penalizing

models that have more parameters, thereby offsetting any improvement in the maximum likelihood allowed by the additional parameters.

But there are different ways of implementing this idea. The two most commonly used approaches are the AIC, which comes from minimizing the Kullback-Leibler information entropy [40] (which measures the difference between the true distribution and the model distribution), and the Bayes Information Criterion (BIC, defined below), which uses the posterior odds of one model against another presuming that the models are equally favored prior to the data fitting [41].

Having at least two criteria helps because none of them are ideal in all circumstances. For example, extensive Monte Carlo testing has indicated that the AIC tends to favor models that have more parameters than the true model [42, 43]. By contrast, the BIC ever more harshly penalizes over-parameterized models as the number of data points increases. For large datasets, BIC should therefore be preferred, though the AIC remains useful since it gives an upper limit to the number of parameters that ought to be included.

The AIC is defined by the expression  $AIC = \chi^2 + 2k$ , where  $k$  is the number of free parameters. Among two models fitted to the data, the one with the least resulting AIC is assessed as the one more likely to be “true.” The unnormalized confidence that model  $i$  is true is the Akaike weight  $\exp(-AIC_i/2)$ . Informally, model  $i$  has likelihood

$$\mathcal{L}_i = \frac{\exp(-AIC_i/2)}{\exp(-AIC_1/2) + \exp(-AIC_2/2)} \quad (4.1)$$

of being closer to the correct model. The difference  $AIC_2 - AIC_1$  therefore determines the extent to which model  $i$  is favored over the other.

A lesser known alternative, though based on similar arguments, is the Kullback Information Criterion (KIC), which takes into account the fact that the PDF’s of the various competing models may not be symmetric. The unbiased estimator for the symmetrized version [44] is given by  $KIC = \chi^2 + 3k$ , very similar to the AIC, but clearly strengthening the dependence on the number of free parameters (from  $2k$  to  $3k$ ). The strength of the evidence in KIC is similar to that for AIC, and the likelihood is calculated using the same Equation (4.1), though with  $AIC_i$  replaced with  $KIC_i$ . The best known of the three is the Bayes Information Criterion (BIC), which represents an asymptotic ( $N \rightarrow \infty$ ) approximation to the outcome of a conventional Bayesian inference procedure for deciding between models [41]. This criterion is defined by  $BIC = \chi^2 + (\ln N)k$ , and clearly suppresses overfitting very strongly if the number of data points  $N$  is large.

We can now proceed to estimate the likelihood of either  $R_h = ct$  or  $\Lambda$ CDM being closer to the correct cosmology, based on fits to the AGN HD in the previous section. From the AIC, we infer that the likelihood of  $R_h = ct$  being the correct cosmology is  $\sim 74\%$  compared to only  $\sim 26\%$  for  $\Lambda$ CDM. The KIC results in a somewhat stronger indication, with a likelihood of  $\sim 89\%$  that  $R_h = ct$  is correct, compared to  $\sim 11\%$  for  $\Lambda$ CDM. The BIC produces the strongest result, mainly because the number of data points is quite large. According to this criterion,  $R_h = ct$  is  $\sim 93\%$  versus  $\sim 7\%$  more likely to be correct than  $\Lambda$ CDM.

It is important to emphasize the fact that these results are fully consistent with, and strongly reinforce, previous results using other observations. For example, based on the cosmic chronometer data, we found that the likelihood of  $R_h = ct$  being closer than  $\Lambda$ CDM to the correct cosmology is  $\sim 82 - 91\%$  versus  $\sim 9 - 18\%$  [36]; from the GRB Hubble Diagram, we found that  $R_h = ct$  is more likely than  $\Lambda$ CDM to be correct with a likelihood of  $\sim 85 - 96\%$  versus  $\sim 4 - 15\%$  [4]; from the high- $z$  quasar Hubble Diagram, we inferred a

relative likelihood of  $\sim 70\%$  versus  $\sim 30\%$  in favor of  $R_h = ct$  [52]; and from the cluster gas mass fraction data, we found this ratio to be  $\sim 95\%$  over  $\sim 5\%$  [45].

## 5 Conclusions

The work reported in this paper has the potential of impacting one of the most important results of Type Ia SN studies—that the Universe is currently experiencing a phase of accelerated expansion—because the two data sets will cover essentially the same redshift range ( $0 \lesssim z \lesssim 2$ ). In this paper, we have demonstrated that the current AGN data already favor the  $R_h = ct$  Universe over  $\Lambda$ CDM. However, the expansion rate in this Universe is constant; the Universe experienced no early deceleration, nor a current acceleration. The Type Ia SN claim of a transition from one to the other is therefore not confirmed by the AGN HD.

Which data should we trust more? Without question, the AGN observations are not yet precise enough to challenge Type Ia SNe. The scatter seen in the AGN Hubble Diagram (Figure 1) is far too large. It is possible that when the refinements and improvements discussed above are implemented, the results described in this paper will change qualitatively, bringing the AGN HD more in line with the Type Ia SN results.

However, the AGN data do not stand alone. As we have documented in several other papers, and summarized above, all of the comparative tests carried out thus far between  $R_h = ct$  and  $\Lambda$ CDM clearly favor the former over the latter. The BIC, in particular, consistently shows that the likelihood of  $R_h = ct$  being correct is an overwhelming  $\gtrsim 95\%$  compared to only  $\lesssim 5\%$  for  $\Lambda$ CDM.

What then are we to make of the Type Ia SN results? The truth is that unlike the cosmic chronometers and the AGN HD, the Type Ia SN data cannot be reduced independently of the pre-assumed cosmological model. The four so-called “nuisance” parameters used to match the SN characteristics to a standard candle must be optimized along with the free parameters of the adopted background cosmology which, up until now, has always been  $\Lambda$ CDM. The inherent weakness of this approach, and the negative impact of trying to use these model-dependent data for comparative studies, have been described in greater detail in ref. [46]. The bottom line is that if it turns out that the Universe is expanding at a constant rate, then trying to fit the Type Ia SN data with  $\Lambda$ CDM is equivalent to attempting a cubic polynomial fit to a straight line: it is impossible to fit the linear dependence perfectly, and the apparent transition from an early deceleration to a current acceleration may simply be the negative consequence of this imperfect polynomial approximation. In view of all the evidence now available from other data, the Type Ia SN data must be recalibrated for  $R_h = ct$  in order to complete a proper comparative test between this cosmology and  $\Lambda$ CDM. We ourselves have recently completed such a test using the Union2.1 SN sample [47, 48], and have reported the results in refs. [49]. The direct one-on-one comparison between  $R_h = ct$  and  $\Lambda$ CDM using this sample shows that both models fit the data with the same  $\chi_{\text{dof}}^2$ . This in itself is quite important because it suggests that the optimization of the nuisance parameters, along with the model, make the data somewhat compliant to the assumed cosmology. The data reduced with one model are not the same as those associated with another; yet each set is fit equally well by its corresponding model. The conclusion that the Universe is accelerating is therefore heavily model dependent. But more than this, as we have found in this paper, the AIC, KIC, and (especially) the BIC strongly favour  $R_h = ct$  because it accounts for the measurements with only one free parameter, whereas  $\Lambda$ CDM has several, depending on how one models the dark-energy equation of state.

Having said this, the importance of a high-precision AGN HD extends well beyond the range of redshifts accessible with these sources and the Type Ia SNe. The discourse concerning whether or not the Universe went through a transition from deceleration to acceleration also bears considerably on our interpretation of the cosmic microwave background (CMB) fluctuations, and their correspondence to physics in the early Universe.  $\Lambda$ CDM has had considerable success accounting for the CMB power spectrum, certainly on scales less than a few degrees [50]. Some of the strongest evidence in favor of the standard model comes from our analysis and interpretation of the radiation produced near the surface of last scattering [32]. So one must be wary about too easily discarding a model that has enjoyed this type of success over many years.

But there are good reasons for also continuing to probe the standard model, not only because we still lack a complete understanding of what happened in the first few seconds following the big bang, but also because in spite of its success, the improving precision of our cosmological measurements points to areas of tension between its predictions and the data. In the CMB, for example, there are still unresolved questions concerning the emergence of possible anomalies that may conflict with the excellent fits to the power spectrum on small scales. For example, the angular correlation function of the CMB not only requires significant cosmic variance to bring theory in line with observations but, more tellingly, reveals an absence of any correlation at angles greater than about 60 degrees [51, 52]. This is potentially quite serious because such an absence of angular correlation would be inconsistent with inflationary theory, the bedrock of modern cosmology. Without inflation, however, a standard model with early deceleration and subsequent acceleration would not be able to explain the general uniformity of the CMB—the so-called horizon problem. This is why in concert with improving Type Ia SNe observations, the construction of a precision AGN HD may help answer the question of whether the Universe did in fact go through a transition from deceleration to acceleration, which bears strongly on the scientific justification for taking inflation seriously.

As much as the AGN HD may eventually fulfill its promise, there is, unfortunately, a practical redshift limit beyond which the AGN HD cannot be extended. At least for the foreseeable future, the method proposed by Watson et al. [1] probably cannot be used to extend the quasar HD to  $z \gtrsim 4$ . The problem is that extending the catalog to high redshifts requires substantially longer temporal baselines because (1) redshift increases  $\tau$  due to time dilation effects, and (2) at higher redshifts we observe more luminous AGNs, which have larger BLRs and hence larger rest-frame lags. For example, the  $H\beta$  lag is already  $\sim 2$  years at  $z \sim 2$ . The lag reaches close to a decade at  $z \sim 2.5$ , making this the practical redshift limit for obtaining lags with  $H\beta$ . Strong UV lines, such as C IV 1549 Å, can do better because the BLR is ionization-stratified, so these higher excitation lines are emitted closer to the central source. Thus, C IV lags could in principle be measurable for objects up to  $z \sim 4$ , but almost certainly not beyond  $z \sim 5 - 6$ . For this reason, it will be equally important to continue the refinement of the high- $z$  quasar HD, which is based—not on individual measurements of  $\tau$ , but rather—on the use of an apparently well constrained luminosity function for objects at  $z \gtrsim 6$  [52]. The high- $z$  quasar approach described in that paper therefore has the unique potential of extending cosmological distance measurements to redshifts well beyond any other classes of object considered thus far.

## Acknowledgments

I am grateful to the anonymous referee for a thorough and helpful review. His/her comments have significantly improved this manuscript. I am also very grateful to Amherst College for its support through a John Woodruff Simpson Lectureship, and to ISSI in Bern where some of this work was carried out.

## References

- [1] Watson, D., Denney, K. D., Vestergaard, M. & Davis, T. M., “A New Cosmological Distance Measure Using Active Galactic Nuclei,” *ApJ Lett*, **740**, L49 (2011)
- [2] Riess, A. G. et al., “Observational Evidence from Supernovae for an Accelerating Universe and a Cosmological Constant,” *AJ*, **116**, 1009 (1998)
- [3] Perlmutter, S. et al., “Measurements of Omega and Lambda from 42 High-Redshift Supernovae,” *ApJ*, **517**, 565 (1999)
- [4] Wei, J.-J., Wu, X. & Melia, F., “The Gamma-ray Burst Hubble Diagram and its Implications for Cosmology,” *ApJ*, **772**, 43 (2013)
- [5] Melia, F., “The High- $z$  Quasar Hubble Diagram,” *JCAP*, **01**, 027 (2014)
- [6] Willott, C. J. et al., “Eddington-limited Accretion and the Black Hole Mass Function at Redshift 6,” *AJ*, **140**, 546 (2010)
- [7] De Rosa, G., Decarli, R., Walter, F., Fan, X., Jiang, L., Kurk, J., Pasquali, A. & Rix, H. W., “Evidence for Non-evolving Fe II/Mg II Ratios in Rapidly Accreting  $z \sim 6$  QSOs,” *ApJ*, **739**, 56 (2011)
- [8] Mortlock, D. J. et al., “A luminous quasar at a redshift of  $z = 7.085$ ,” *Nature*, **474**, 616 (2011)
- [9] Baldwin, J. A., “Luminosity Indicators in the Spectra of Quasi-Stellar Objects,” *ApJ*, **214**, 679 (1977)
- [10] Collier, S., Horne, K., Wanders, I. & Peterson, B. M., “A new direct method for measuring the Hubble constant from reverberating accretion discs in active galaxies,” *MNRAS*, **302**, L24 (1999)
- [11] Elvis, M. & Karovska, M., “Quasar Parallax: A Method for Determining Direct Geometrical Distances to Quasars,” *ApJ Letters*, **581**, L67 (2002)
- [12] Marziani, P., Sulentic, J. W., Zamanov, R. et al., “Using Quasars for Cosmology,” *Mem. Soc. Astron. Ital.*, **3**, 218 (2003)
- [13] Blandford, R. D. & McKee, C. F., “Reverberation mapping of the emission line regions of Seyfert galaxies and quasars,” *ApJ*, **255**, 419 (1982)
- [14] Peterson, B. M., Ferrarese, L., Gilbert, K. M. et al., “Central Masses and Broad-Line Region Sizes of Active Galactic Nuclei. II. A Homogeneous Analysis of a Large Reverberation-Mapping Database,” *ApJ*, **613**, 682 (2004)
- [15] Bentz, M. C., Peterson, B. M., Netzer, H., Pogge, R. W. & Vestergaard, M., “The Radius-Luminosity Relationship for Active Galactic Nuclei: The Effect of Host-Galaxy Starlight on Luminosity Measurements. II. The Full Sample of Reverberation-Mapped AGNs,” *ApJ*, **697**, 160 (2009)
- [16] Bentz, M. C., Denney, K. D., Grier, C. J. et al., “The Low-luminosity End of the Radius-Luminosity Relationship for Active Galactic Nuclei,” *ApJ*, **767**, 149 (2013)
- [17] Bentz, M. C., Walsh, J. L., Barth, A. J. et al., “The Lick AGN Monitoring Project: Broad-line

- Region Radii and Black Hole Masses from Reverberation Mapping of H $\beta$ ,” ApJ, **705**, 199 (2009)
- [18] Kaspi, S., Smith, P. S., Netzer, H., Maoz, D., Jannuzi, B. T. & Givon, U., “Reverberation Measurements for 17 Quasars and the Size-Mass-Luminosity Relations in Active Galactic Nuclei,” ApJ, **533**, 631 (2000)
- [19] Kaspi, S., Maoz, D., Netzer, H. et al., “The Relationship between Luminosity and Broad-Line Region Size in Active Galactic Nuclei,” ApJ, **629**, 61 (2005)
- [20] Zu, Y., Kochanek, C. S., Peterson, B. M., “An Alternative Approach to Measuring Reverberation Lags in Active Galactic Nuclei,” ApJ, **735**, 80 (2011)
- [21] Denney, K. D., Peterson, B. M., Pogge, R. W. et al., “Reverberation Mapping Measurements of Black Hole Masses in Six Local Seyfert Galaxies,” ApJ, **721**, 715 (2010)
- [22] Schlegel, D. J., Finkbeiner, D. P. & Davis, M., “Maps of Dust Infrared Emission for Use in Estimation of Reddening and Cosmic Microwave Background Radiation Foregrounds,” ApJ, **500**, 525 (1998)
- [23] Schlafly, E. F., Finkbeiner, D. P., Schlegel, D. J. et al., “The Blue Tip of the Stellar Locus: Measuring Reddening with the Sloan Digital Sky Survey,” ApJ, **725**, 1175 (2010)
- [24] Baldwin, J., Ferland, G., Korista, K. & Verner, D., “Locally Optimally Emitting Clouds and the Origin of Quasar Emission Lines,” ApJL, **455**, L119 (1995)
- [25] Tonry, J. L., Dressler, A., Blakeslee, J. P. et al., “The SBF Survey of Galaxy Distances. IV. SBF Magnitudes, Colors, and Distances,” ApJ, **546**, 681 (2001)
- [26] Cackett, E. M., Horne, K. & Winkler, H., “Testing thermal reprocessing in active galactic nuclei accretion discs,” MNRAS, **380**, 669 (2007)
- [27] Melia, F., “The Cosmic Horizon,” MNRAS, **382**, 1917 (2007)
- [28] Melia, F. & Shevchuk, A., “The  $R_h = ct$  Universe,” MNRAS, **419**, 2579 (2012)
- [29] Weyl, H., “Zue Allgemeinen Relativitatstheorie,” Z. Phys., **24**, 230 (1923)
- [30] Milne, E. A., “World-Structure and the Expansion of the Universe. Mit 6 Abbildungen,” Zeitschrift für Astrophysik, **6**, 1 (1933)
- [31] Riess, A. et al., “A 3% Solution: Determination of the Hubble Constant with the Hubble Space Telescope and Wide Field Camera 3,” ApJ, **730**, id. 119 (2011)
- [32] Planck Collaboration, Ade, P.A.R. et al., “Planck 2013 results. XVI. Cosmological parameters,” A&A in press (arXiv:1303.5076)
- [33] Komatsu, E., Smith, K. M., Dunkley, J. et al., “Seven-year Wilkinson Microwave Anisotropy Probe (WMAP) Observations: Cosmological Interpretation,” ApJS, **192**, 18 (2011)
- [34] Kessler, R., Becker, A. C., Cinabro, D. et al., “First-Year Sloan Digital Sky Survey-II Supernova Results: Hubble Diagram and Cosmological Parameters,” ApJS, **185**, 32 (2009)
- [35] Conley, A., Guy, J., Sullivan, M. et al., “Supernova Constraints and Systematic Uncertainties from the First Three Years of the Supernova Legacy Survey,” ApJS, **192**, 1 (2011)
- [36] Melia F. & Maier, R., “Cosmic Chronometers in the  $R_h = ct$  Universe,” MNRAS, **432**, 2669 (2013)
- [37] Liddle, A. R., “How many cosmological parameters?” MNRAS, **351**, L49 (2004)
- [38] Liddle, A. R., “Information criteria for astrophysical model selection,” MNRAS, **377**, L74 (2007)
- [39] Tan, M. Y. J. & Biswas, R., “The reliability of the Akaike information criterion method in cosmological model selection,” MNRAS, **419**, 3292 (2012)

- [40] Takeuchi, T. T., “Application of the Information Criterion to the Estimation of Galaxy Luminosity Function,” *Ap. Space Sci.*, **271**, 213 (2000)
- [41] Schwarz, G., “Estimating the Dimension of a Model,” *Ann. Statist.*, **6**, 461 (1978)
- [42] Harvey, A. C., “Time Series Models,” Prentice Hall, Hertfordshire (1993)
- [43] Kass, R. E. & Raftery, A. E., “Bayes Facators,” *J. American Stat. Assoc.*, **90**, 773 (1995)
- [44] Cavanaugh, J. E., “A large-sample model selection criterion based on Kullback’s symmetric divergence,” *Statist. Probab. Lett.*, **42**, 333 (1999)
- [45] Melia, F., “The Cluster Gas Mass Fraction in the  $R_h = ct$  Universe,” PRD, submitted (2013)
- [46] Melia, F., “Fitting the Union2.1 Supernova Sample with the  $R_h = ct$  Universe,” *AJ*, **144**, article id. 110 (2012)
- [47] Kowalski, M. R. et al., “Improved Cosmological Constraints from New, Old, and Combined Supernova Data Sets,” *ApJ*, **686**, 749 (2008)
- [48] Suzuki, N. et al., “The Hubble Space Telescope Cluster Supernova Survey. V. Improving the Dark-energy Constraints above  $z > 1$  and Building an Early-type-hosted Supernova Sample,” *ApJ*, **746**, 85 (2012)
- [49] Wei, J.-J., Wu, X. & Melia, F., “A Comparative Analysis of the Union2.1 SN Sample with LCDM and the  $R_h = ct$  Universe,” *AJ*, in press (2014)
- [50] Bennett, C. L. et al., “Seven-year Wilkinson Microwave Anisotropy Probe (WMAP) Observations: Are There Cosmic Microwave Background Anomalies?” *ApJS*, **192**, Article ID 17 (2011)
- [51] Copi, C. J., Huterer, D., Schwarz, D. J. & Starkman, G. D., “Large-Angle Anomalies in the CMB,” *Adv. Astr.*, 2010, id. 847541 (2010)
- [52] Melia, F., “Angular correlation of the cosmic microwave background in the  $R_h = ct$  Universe,” *A& A*, 561, id.A80 (2014)